RC23818 (W0512-002) December 1, 2005
Chemistry

IBM Research Report

Electrodeposition of Gold on Silicon

Q. Huang, H. Deligianni, L. T. Romankiw
IBM Research Division
Thomas J. Watson Research Center
P.O. Box 218
Yorktown Heights, NY 10598

Research Division
Almaden - Austin - Beijing - Haifa - India - T. J. Watson - Tokyo - Zurich

LIMITED DISTRIBUTION NOTICE: This report has been submitted for publication outside of IBM and will probably be copyrighted if accepted for publication. Ithas been issued as a Research Report for early dissemination of its contents. In view of the transfer of copyright to the outside publisher, its distributionoutside of IBM prior to publication should be limited to peer communications and specific requests. After outside publication, requests should be filled only by reprints or legally obtained copies of the article (e.g, payment of royalties). Copies may be requested from IBM T. J. Watson Research Center , P. O. Box 218, Yorktown Heights, NY 10598 USA (email: reports@us.ibm.com). Some reports are available on the internet at http://domino.watson.ibm.com/library/CyberDig.nsf/home

Electrodeposition of Gold on Silicon

Q. Huang, H. Deligianni[z], L. T. Romankiw

IBM, T. J. Watson Research Center
P.O. Box 218, Yorktown Heights, NY 10598

Abstract

Gold electrodeposition on n-Si (100) surface was investigated by performing a detailed study on nucleation and growth. With addition of thallium in the solution, enhancement and inhibition of the gold deposition were observed at low potential and high potential, respectively. The nucleation of gold on Si was found to depend on the Au concentration and applied potential as well as the Tl^+ addition. At low current densities Tl^+ increases the Au nuclei size and decreases the density by catalyzing the nuclei growth. At high current densities, an opposite effect was observed. An adsorbed thallium intermediate species is proposed to explain both the catalytic and suppressive effects.

Introduction

Compared to metal electrodeposition on metal substrates, the electrodeposition on semiconductors is different at two aspects, the semiconductor characteristics of the substrate and the weak interaction between the semiconductor material and most metal species. In contrast to the continuous electron energy levels in metals, the electron energy levels in semiconductor form two energy bands, valence band and conduction band, which are separated by a certain energy gap, the band gap. Furthermore, due to the limited number of carriers available in semiconductor, the charge in the substrate is

[z] Email: lili@us.ibm.com

distributed across a space charge region instead of a surface charge layer in metal substrate. The semiconductor-electrolyte interface forms a Schottky barrier, similar to most metal-semiconductor contacts, except that the work function of the metal is substituted by the Fermi level of the redox couple in electrolyte. Therefore, at equilibrium and depletion conditions, a fluctuation in the applied potential only changes the charge distribution across the space charge region, or the band bending, while the potential drop across the Helmholtz layer remains constant. Only when a significant cathodic (for n-type Si) current flows from the semiconductor substrate to the electrolyte, the potential across the Helmholtz layer changes [1].

In addition to the semiconducting nature of the substrate, metal electrodeposition on semiconductors is also complicated by the nucleation process. Due to the weak interaction between the metal and the semiconductor, the metal nucleation follows the Volmer-Weber mechanism, an island formation and transport controlled 3-D growth process. This process can occur with electrodeposition on foreign substrates when the interaction between deposit and substrate is weak. The mechanism has been extensively studied and the two extreme cases, instantaneous and progressive nucleation, have been well described [2-4].

In spite that metal electrodeposition on semiconductor substrates might allow the direct formation of Schottky contact and the direct integration of metal electrodeposition with other semiconductor processes, this subject has not been addressed until recently a few groups reported some studies on different systems [5-17]. Among them, Depestel and Strubbe [5] studied the Au nucleation on GaAs in a cyanide-based alkaline chemistry and found that the nucleation depended strongly on the crystal orientation of GaAs

[z] Email: lili@us.ibm.com

substrate, probably due to the different chemical composition on the different crystal surfaces. Oskam et al. studied the Au electrodeposition on Si in a similar chemistry, where a progressive nucleation was observed [10,18,19]. They plated a high quality Si/Au Schottky structure with a pulse scheme, where a high potential nucleation pulse was followed by a low potential for film growth [18]. More recently, the effect of iodide ion was studied on Au electrodeposition on a glassy carbon electrode. A high nucleation density and a preferred Au(111) orientation were observed [20]. In this report, our studies are focused on the effect of thallium addition on Au deposition on n-Si. The effects of thallium on Au bulk film electrodeposition as well as on the initial nucleation stages were investigated.

Experimental

Experiments were carried out in a traditional three-electrode cell, with a platinum mesh as counter electrode and a saturated calomel electrode (SCE) as reference. The working electrode is a rotating disk electrode (RDE), in which a Si piece was mounted. The Si wafers used were antimony doped n-Si(100) with resistivity between 0.008 to 0.03 Ω·cm. The Si pieces were cleaned by a standard Huang clean process to remove organic contamination and surface oxide. A dilute HF dip for 1 minute followed by ethanol rinse and nitrogen dry was carried out immediately before the Si was mounted into the RDE for electrodeposition. InGa eutectic was used to ensure the ohmic contact.

Neutronex® 309 Au solution from Cookson Electronics Inc, a sulfite based Au chemistry, was used as the gold solution make-up. Solutions with desired Au concentration were obtained by diluting the original solution, with pH kept between 9.0 and 9.3. Reagent graded thallium(I) acetate, $Tl(OOCCH_3)$, from Aldrich Inc was used as

[z] Email: lili@us.ibm.com

an additive for Au electrodeposition. An EG&G 273 potentiostat by Princeton Research Inc was used as a power source for most of the electrochemical studies. The nucleation studies were performed using an AutoLab PGSTAT30 by Eco Chemie LLC by applying a short cathodic pulse on a high impedance Si substrate. All experiments in this report were carried out at room temperature.

Results and Discussion

Figure 1 shows two cyclic voltammograms in a 5 mM Au electrolyte at 1000 rpm on n-Si and Au disk electrodes, respectively. A scan rate of 200 mV/sec was used to avoid surface area deviation due to significant Au deposition. No underpotential deposition was observed for Au electrodeposition on Si due to the weak interaction between Au and Si. On the contrary, a nucleation overpotential of -0.4 V was observed, suggesting that Au electrodeposition occurs preferentially on Au over Si. After the Si surface was completely covered with the plated Au after first scan, the plating became identical to Au electrode at low potential. At high potential, the electrodeposition current on Si was significantly lower than the Au electrode, due to the higher resistivity of the Si substrate.

In order to study the effect of thallium on the Au electrodeposition on Si, polarization was carried out in electrolytes with different amount of thallium(I) acetate at the same conditions as Figure 1. The first scan is presented in Figure 2. At a potential more positive than -1.4 V vs. SCE, the addition of Tl increases the current density. As the Tl concentration increases, this current enhancement becomes more pronounced and reaches a "saturation" at 10 ppm Tl, for which a current peak was observed at around -1.1 V vs. SCE. In a Au-free electrolyte, with only Tl and Na_2SO_4 supporting salts, a constant

[z] Email: lili@us.ibm.com

but negligibly small current was observed at low potential up to -1.5 V vs. SCE, clearly indicating that there is no significant electrochemical reaction of Tl on Si. Studies in different electrolytes and different agitation conditions showed that the peak current was proportional to the square root of the rotation speed and to the Au concentration, indicative of mass transport control of Au plating. In this potential range, the presence of Tl greatly catalyzes the Au electrodeposition kinetics, resulting in a mass transport limited system.

Potentiostatic deposition was carried out at -1.1 V vs. SCE at 1000 rpm and the current densities as a function of time are shown in Figure 3(a). A same constant current was again observed for electrolytes with 10 ppm Tl or more. The deposition rates obtained from weight difference measurements, 0.04, 0.12, 0.18 and 0.18 mg/(cm^2·min) for electrolytes with 0, 2, 10, and 18 ppm Tl, respectively, are perfectly consistent with the conclusion that Au deposition was facilitated by Tl and that the limiting current was reached at this potential when the Tl concentration reaches 10 ppm. Film composition was analyzed by photon induced x-ray emission (PIXE). For the film plated with 18 ppm Tl addition, the Tl inclusion was determined as 0.4±0.5 at.%. It is believed that thallium catalyzes the Au deposition, without being co-deposited.

The films from the potentiostatic deposition were also characterized with scanning electron microscopy (SEM), as shown in Figures 3 (b) to (e). The addition of Tl in the electrolyte increases the surface roughness. In the extreme case of 18 ppm Tl, tree-shaped gold deposits were plated. It is well known that mass transport controlled electrodeposition generally increases the surface roughness and results in dendritic growth. However, the gold electrodeposition current density in the presence of 18 and 10

[z] Email: lili@us.ibm.com

ppm of Tl were the same while the deposits were much different. Our hypothesis is that a catalytic Tl species adsorbs onto the electrode surface and, based upon its coverage, it catalyzes the Au deposition rate. The local variation in the coverage of the adsorbed Tl species causes a difference in the local deposition rate, resulting in a tree-shaped deposit.

Figure 4 shows the scans after the first scan in cyclic voltammograms of Au electrodeposition on Si with different amount of Tl. Comparison of the voltammograms in Figures 2 and 4 shows that the current peak in the first scan is always lower than the ones in subsequent scans. The cathode surface was initially Si and was converted to Au surface by the subsequent deposition. The lower peak current in the first scan suggests that the catalytic effect of Tl on Au deposition on Au is more pronounced than Au deposition on Si. In other words, the Au deposits more preferentially on Au over Si at the low potential range in the presence of Tl^+.

In addition to the deposition rate enhancement at low potential, it is also evident in Figure 4 that the presence of Tl decreases the Au deposition rate at high potential. This current suppression becomes more pronounced as the Tl concentration increases in the electrolyte, and the suppression does not "saturate" even at 18 ppm Tl. Furthermore, comparison of Figures 2 and 4 shows that this inhibition effect is more evident on the Au than on the Si surface. Potentiostatic deposition was also carried out at -2 V vs. SCE at different Tl concentration for composition analysis with PIXE. The Tl contents were 0±0.5 at.% and 2.7±0.5 at.% for the deposits with the presence of 2 ppm and 18 ppm Tl in the electrolyte, respectively. The suppression of Au electrodeposition at high potential is believed to result from the co-deposition of Tl. The higher the Tl concentration in the

[z] Email: lili@us.ibm.com

electrolytes, the higher Tl incorporation in the deposit, and the more pronounced the current suppression at high potentials.

Electrodeposition of Tl^+ on Au electrodes was studied decades ago and an underpotential deposition (UPD) mechanism was suggested [21]. The deposition potential shift was up to 0.69 V in an acidic Au solution due to the very strong interaction between Au and Tl atoms [21, 22]. In this study, an adsorbed Tl intermediate apparently catalyzes the deposition of Au on Au surface at low potentials. As the potential increases, the adsorbate is further reduced into Tl atoms. Consequently, the Au electrodeposition becomes no more catalyzed, and the current drops at around -1.5 V vs. SCE in the cyclic voltammograms (Figures 2 and 4). At the same time, the Tl atom starts to incorporate into the Au deposit, resulting in the suppressed Au deposition.

The effect of Tl on the Au nucleation on Si was studied and Figure 5 shows the nucleation densities and the SEM micrographs at different galvanostatic plating in absence and presence of 18 ppm Tl^+. A rotation rate of 1000 rpm was used. In either thallium-free or thallium-containing electrolytes, higher current density results in smaller nuclei and higher nucleation density, as expected from the nucleation overpotential observed for Au deposition on Si (Figure 1). Comparison of the two electrolytes shows that the presence of 18 ppm Tl^+ significantly changed the Au nucleation on Si. When a low current density is applied, such as -1 mA/cm^2, the nuclei size is increased and the nucleation density is decreased by Tl^+, shown in Figures 5 (b) and (e). The previous discussion showed that the Au plating at low potential was catalyzed by Tl^+ on Au but not on Si (Figures 2 and 4). Therefore, once a Au particle forms, the subsequent Au

[z] Email: lili@us.ibm.com

deposition preferably occurs on the Au particle in galvanostatic plating, resulting in a larger particle size and a lower nucleation density.

On the contrary, Au deposition on Au is suppressed at a high potential due to the co-deposition of Tl, and this suppression was less pronounced for Au deposition on Si. Consequently, galvanostatic plating at a high current density, such as -10 mA/cm^2, in a Tl-containing electrolyte is expected to result in a higher nucleation density than Tl-free electrolyte, as prooved in Figures 5 (d) and (g). At a medium current, such as -5 mA/cm^2, shown in Figures 5 (c) and (f), no significant difference was observed for the nucleation in the absence and presence of Tl^+. The effects of Tl^+ on Au nucleation density are summarized in Figure 5(a). The highest nucleation density of 2×10^{11} cm^{-2} was achieved at high current densities when 18 ppm Tl^+ was present.

Due to the weak interaction between metal and Si substrate, metal deposition on Si follows the Volmer-Weber model, an island formation and a mass transport controlled 3-D growth process. For the two extreme cases, ideal progressive and instantaneous nucleation, the current transient response for a potential step on a stagnant electrode is described by the following equations [2]:

$$i(t) = \frac{z \cdot F \cdot D^{1/2} \cdot c}{\pi^{1/2} \cdot t^{1/2}} \left[1 - \exp\left(-N \cdot \pi \cdot k \cdot D \cdot t\right)\right] \qquad \text{instantaneous nucleation}$$

$$i(t) = \frac{z \cdot F \cdot D^{1/2} \cdot c}{\pi^{1/2} \cdot t^{1/2}} \left[1 - \exp\left(-\frac{1}{2} \cdot A \cdot N_{\infty} \cdot \pi \cdot k' \cdot D \cdot t^2\right)\right] \qquad \text{progressive nucleation}$$

[z] Email: lili@us.ibm.com

where $k = \left(\frac{8 \cdot \pi \cdot c \cdot M}{\rho} \right)^{1/2}$ and $k' = \frac{4}{3}\left(\frac{8 \cdot \pi \cdot c \cdot M}{\rho} \right)^{1/2}$. A simplified form can be obtained by nondimensionalizing the current and time with the values at maximum current, $i_{\max}$ and $t_{\max}$ [2, 3].

$$i(t)/i_{\max} = \left\{ \frac{1.9542}{\left(t/t_{\max} \right)} \left[1 - \exp\left(-1.2564 \; t/t_{\max} \right) \right]^2 \right\}^{1/2} \qquad \text{instantaneous nucleation}$$

$$i(t)/i_{\max} = \left\{ \frac{1.2254}{\left(t/t_{\max} \right)} \left[1 - \exp\left(-2.3367 \left(t/t_{\max} \right)^2 \right) \right]^2 \right\}^{1/2} \qquad \text{progressive nucleation}$$

Figures 6 (a) and (b) show the stagnant chronoamperometry in 5 mM Au electrolytes without and with 18 ppm Tl^+, respectively. At a potential more negative than -0.65 V vs. SCE a current peak was observed in the thallium-free electrolyte, after which the current decays to the same value for all potentials. In the presence of 18 ppm Tl, not only a significantly higher peak current but also a delay of the peak current was observed, suggesting the adsorption of Tl^+ during the Au electrodeposition.

The dimensionless current transients were re-plotted in Figures 7 (a) and (b) for the potentials where a current maxima were observed. The ideal progressive and instantaneous nucleation cases were included for comparison. It can be seen that the nucleation in a thallium-free 5 mM Au electrolyte at low potential, -0.675 V to -0.725 V vs. SCE, is between the progressive and instantaneous cases. When the potential reaches -0.75 V vs. SCE, the current transient falls out of the range of the two extreme cases,

[z] Email: lili@us.ibm.com

indicative of other side reactions. On the contrary, the presence of 18 ppm Tl^+ results in a current transient outside the two extreme cases for all the potentials studied. In general, the current is higher than the instantaneous nucleation before the current maxima but lower than the progressive case after the maxima, consistent with an adsorption-saturation hypothesis of the Tl adsorbate on Au.

Chronoamperometry was also carried out in a Tl-free electrolyte with 1 mM Au, shown in Figures 8 (a) and (b). For potentials higher than -0.8 V vs. SCE, the nucleation was found to be close to an instantaneous process. Figures 9 (a) and (b) show SEM micrographs for Au deposition at -10 mA/cm^2 in this dilute Au electrolyte. The nucleation density in Figure 7(a), 3×10^{11} cm^{-2}, was found much higher than the case of 5 mM Au electrolyte, 6×10^{10} cm^{-2}. As the deposition continues for longer time, a uniform nuclei size was maintained and finally merged with each other. No new nuclei were formed for the 1 mM Au case, consistent with the instantaneous nucleation process observed in the chronoamperometry study.

Conclusions

Electrodeposition of Au on n-Si (100) surface was investigated in a mild alkaline chemistry. Addition of Tl^+ in the electrolyte significantly enhanced the Au deposition rate at low potentials, while the deposition at high potentials is suppressed. An adsorbed Tl intermediate is proposed to explain both the catalytic and the suppressive effects on Au electrodeposition. The nucleation of Au on Si was found dependent on the Au concentration and applied potential. An instantaneous nucleation process was observed for a 1 mM Au electrolyte, while the nucleation was found between instantaneous and progressive processes for 5 mM Au electrolyte. The addition of Tl decreases the

[z] Email: lili@us.ibm.com

nucleation density and increases the nuclei size at low current, while it increases the nucleation density and decreases the size at high current.

Acknowledgements

The authors would like to thank Dr. Guy Cohen for helpful and Dr. Andrew Kellock for composition analysis.

References

1. R. Memming, *Semiconductor Electrochemistry*, Wiley, John & Sons, Weinheim (2001).
2. G. Gunawardena, G. Hills, I. Montenegro and B. Scharifker. *Journal of Electroanalytical Chemistry*, **138**, 225 (1982).
3. B. Scharifker and G. Hills. *Electrochimica Acta*, **28**, 879 (1983).
4. B. Scharifker and J. Mostany. *Journal of Electroanalytical Chemistry*, **177**, 13 (1984).
5. L.M. Depestel and K. Strubbe. *Journal of Electroanalytical Chemistry*, **572**, 195 (2004).
6. H. Gomez, R. Henriquez, R. Schrebler, R. Cordova, D. Ramirez, G. Riveros and E.A. Dalchiele. *Electrochimica Acta*, **50**, 1299 (2005).
7. A. Imanishi, K. Morisawa and Y. Nakato. *Electrochemical and Solid-State Letters*, **4**, C69 (2001).
8. R. Krumm, B. Guel, C. Schmitz and G. Staikov. *Electrochimica Acta*, **45**, 3255 (2000).
9. K. Marquez, G. Staikov and J.W. Schultze. *Electrochimica Acta*, **48**, 875 (2003).

[z] Email: lili@us.ibm.com

10. G. Oskam and P.C. Searson. *Journal of the Electrochemical Society*, **147**, 2199 (2000).

11. G.R. Pattanaik, D.K. Pandya and S.C. Kashyap. *Journal of the Electrochemical Society*, **149**, C363 (2002).

12. B. Rashkova, B. Guel, R.T. Potzschke, G. Staikov and W.J. Lorenz. *Electrochimica Acta*, **43**, 3021 (1998).

13. M. Takahashi, M. Todorobaru, K. Wakita and K. Uosaki. *Applied Physics Letters*, **80**, 2117 (2002).

14. A. Radisic, A.C. West and P.C. Searson. *Journal of the Electrochemical Society*, **149**, C94 (2002).

15. A.A. Pasa and W. Schwarzacher. *Physics Status Solidi A*, **173**, 73 (1999).

16. L.J. Gao, P. Ma, K.M. Novogradecz and P.R. Norton. *Journal of Applied Physics*, **81**, 7595 (1997).

17. A.P. O'keeffe, O.I. Kasyutich, W. Schwarzacher, L.S.d. Oliveira and A.A. Pasa. *Applied Physics Letters*, **73**, 1002 (1998).

18. G. Oskam, D.v. Heerden and P.C. Searson. *Applied Physics Letters*, **73**, 3241 (1998).

19. G. Oskam and P.C. Searson. *Surface Science*, **446**, 103 (2000).

20. M.S. El-Deab, T. Sotomura and T. Ohsaka. *Journal of the Electrochemical Society*, **152**, C1 (2005).

21. D.M. Kolb, in *Advances in Electrochemistry and Electrochemical Engineering*, H. Gerischer and C.W. Tobias, Editors, **11**, 125, Wiley-Interscience, New York, NY (1978).

[z] Email: lili@us.ibm.com

22. D.M. Kolb, M. Przasnyski and H. Gerischer. *Electroanalytical Chemistry and Interfacial Electrochemistry*, **54**, 25 (1974).

[z] Email: lili@us.ibm.com

Figure Captions:

Figure 1. Cyclovoltammograms of 5mM Au solution on n-Si (100): (□) first scan, (■) subsequent scans, and (▲) gold electrodes, sweep rate = 200 mV/sec.

Figure 2. The first scan of the cyclic voltammograms on n-Si (100) electrode in 5mM Au solutions with (●) 0 ppm, (□) 10 ppm and (▲) 18 ppm Tl in form thallium(I) acetate, sweep rate = 200 mV/sec.

Figure 3. (a) Current - time curves and (b-e) SEM micrographs of the deposits on n-Si (100) for potentiaostatic plating at -1.1 V vs. SCE in 5 mM Au solutions with (●, b) 0 ppm, (○, c) 2 ppm, (□, d) 10 ppm and (▲, e) 18 ppm Tl^{+}.

Figure 4. Scans after the first scan of the cyclic voltammograms on n-Si (100) electrode in 5mM Au solutions with (●) 0 ppm, (□) 10 ppm and (▲) 18 ppm Tl in form thallium(I) acetate, sweep rate = 200 mV/sec.

Figure 5. Nucleation density of galvanostatic plating in n-Si (100) in 5 mM Au solutions: (a) summary, (b, c, d) 0 ppm Tl, at -1, -5, -10 mA/cm^2, (e, f, g) 18 ppm Tl, at -1, -5, -10 mA/cm^2.

Figure 6. Current transients in stagnant potentiostatic plating on n-Si (100) at different potentials in 5 mM Au solutions with (a) 0 ppm and (b) 18 ppm Tl.

Figure 7. Normalized current transients in stagnant potentiostatic plating on n-Si (100) at different potentials in 5 mM Au solutions with (a) 0 ppm and (b) 18 ppm Tl.

Figure 8. (a) Non-normalized and (b) normalized current transients in stagnant potentiostatic plating on n-Si (100) at different potentials in 1 mM Au solution without Tl.

[z] Email: lili@us.ibm.com

Figure 9. SEM micrograph of Au nucleation on n-Si (100) in 1 mM Au solution in galvanostatic plating at -10 mA/cm^2 for (a) 50 and (b) 500 seconds.

[z] Email: lili@us.ibm.com

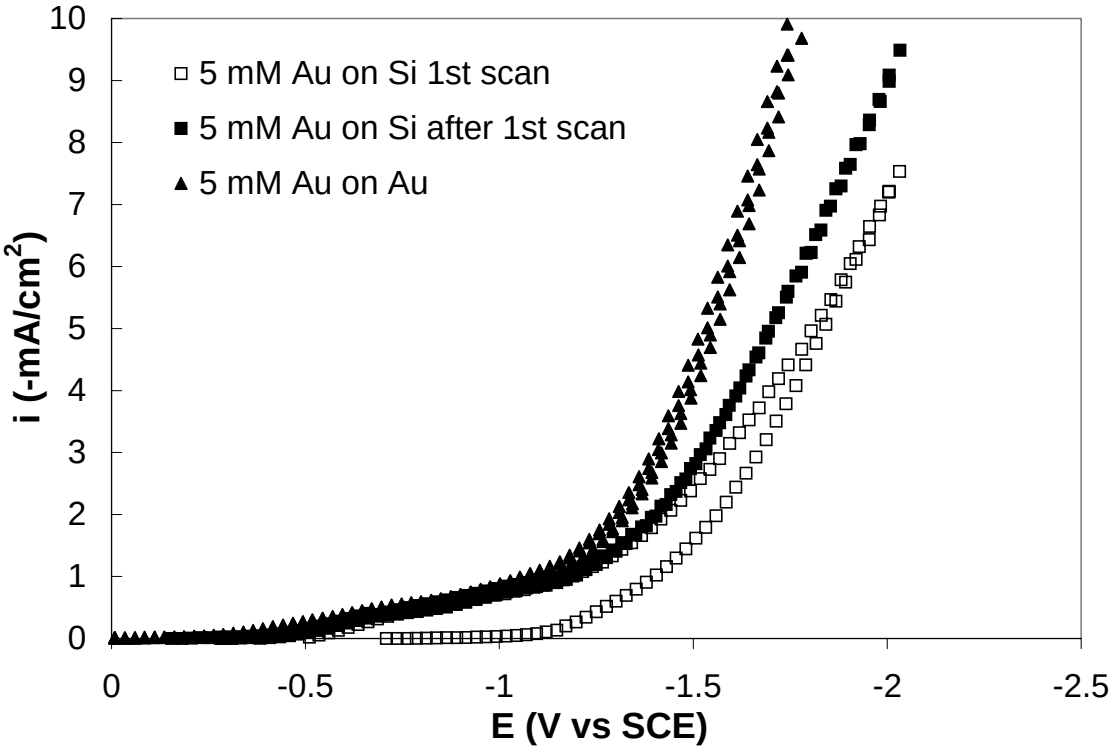

Figure 1.

z Email: lili@us.ibm.com

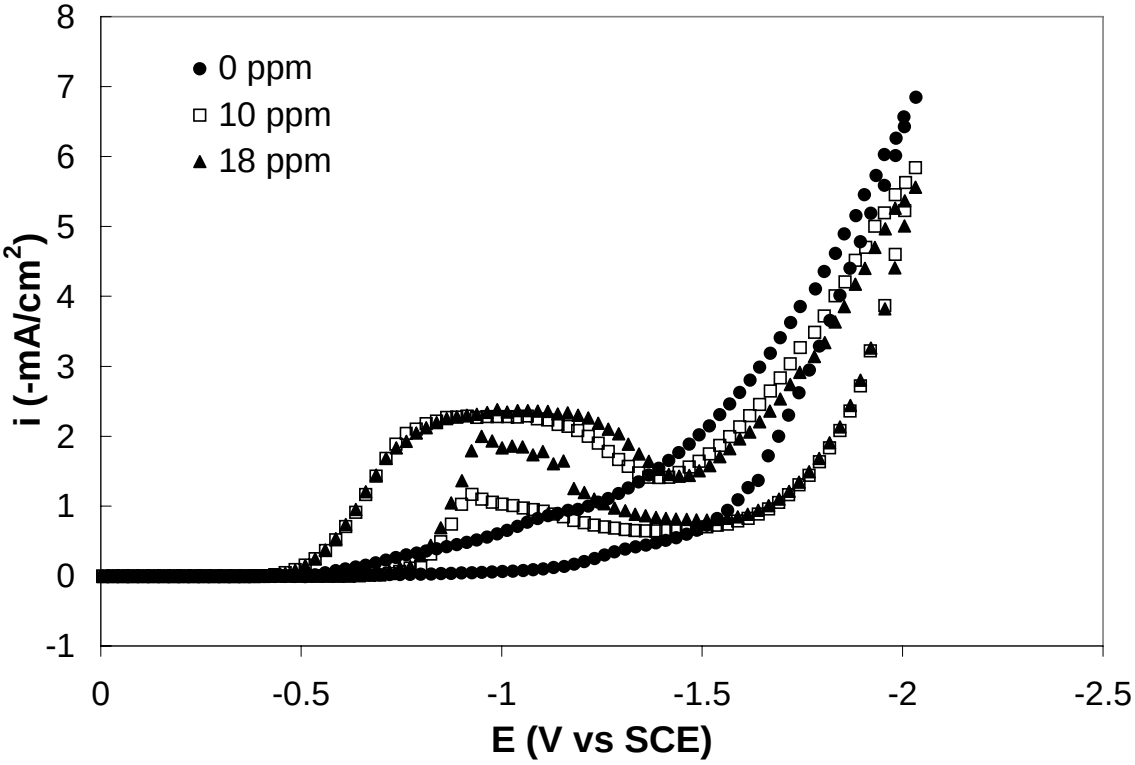

Figure 2.

z Email: lili@us.ibm.com

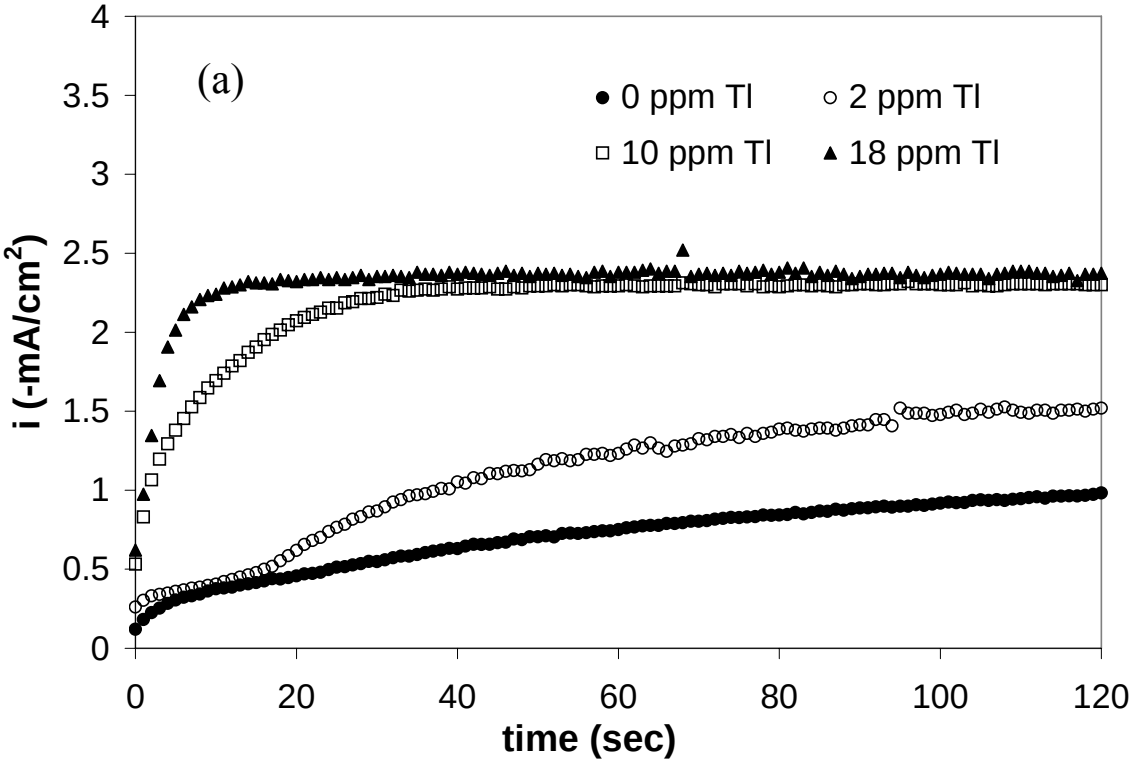

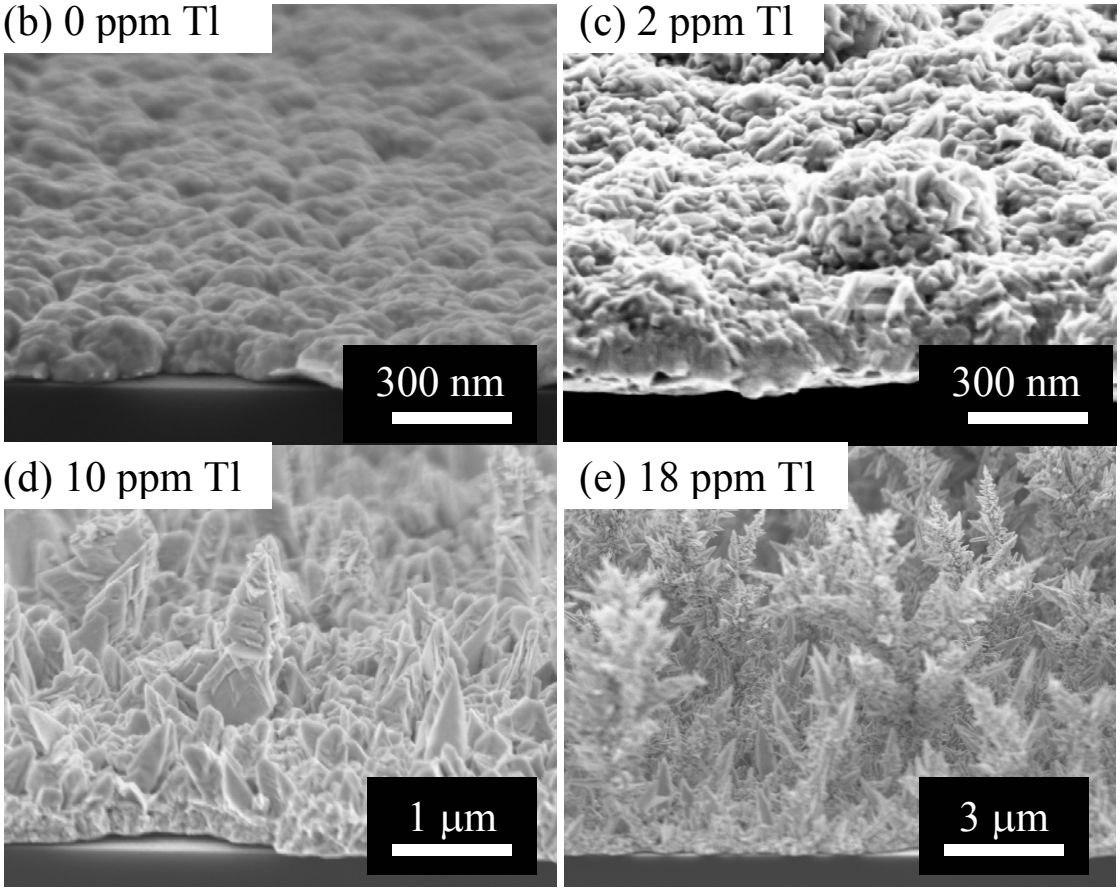

z Email: lili@us.ibm.com Figure 3 (a - e).

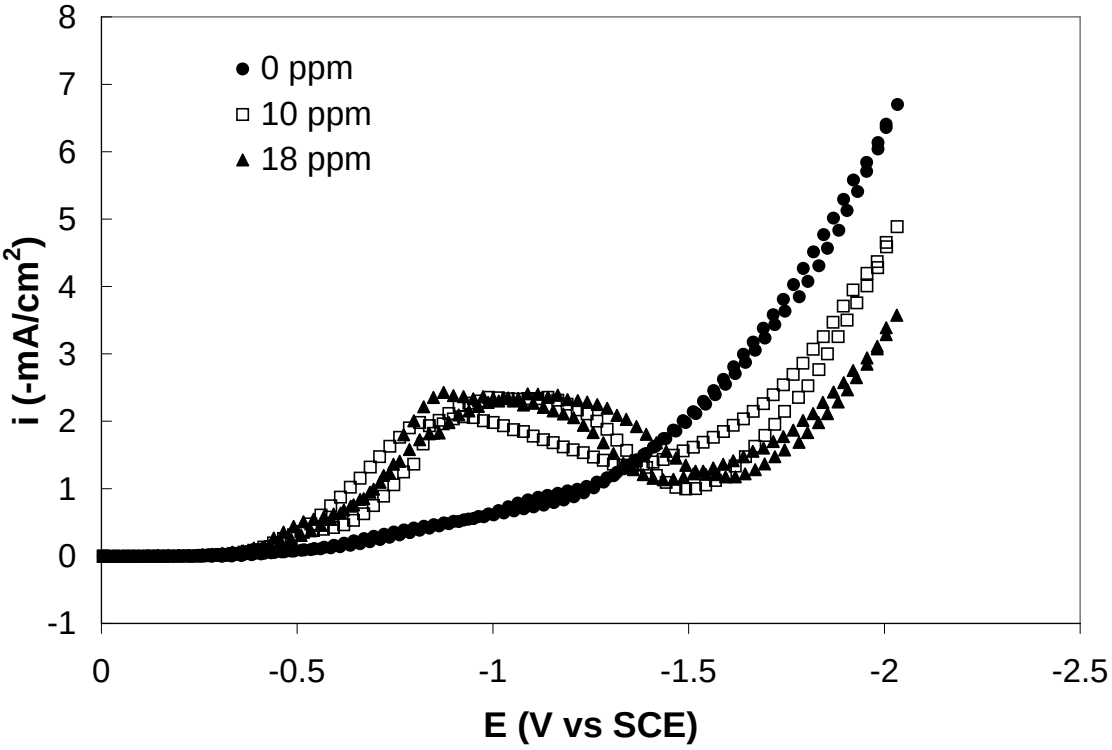

Figure 4.

z Email: lili@us.ibm.com

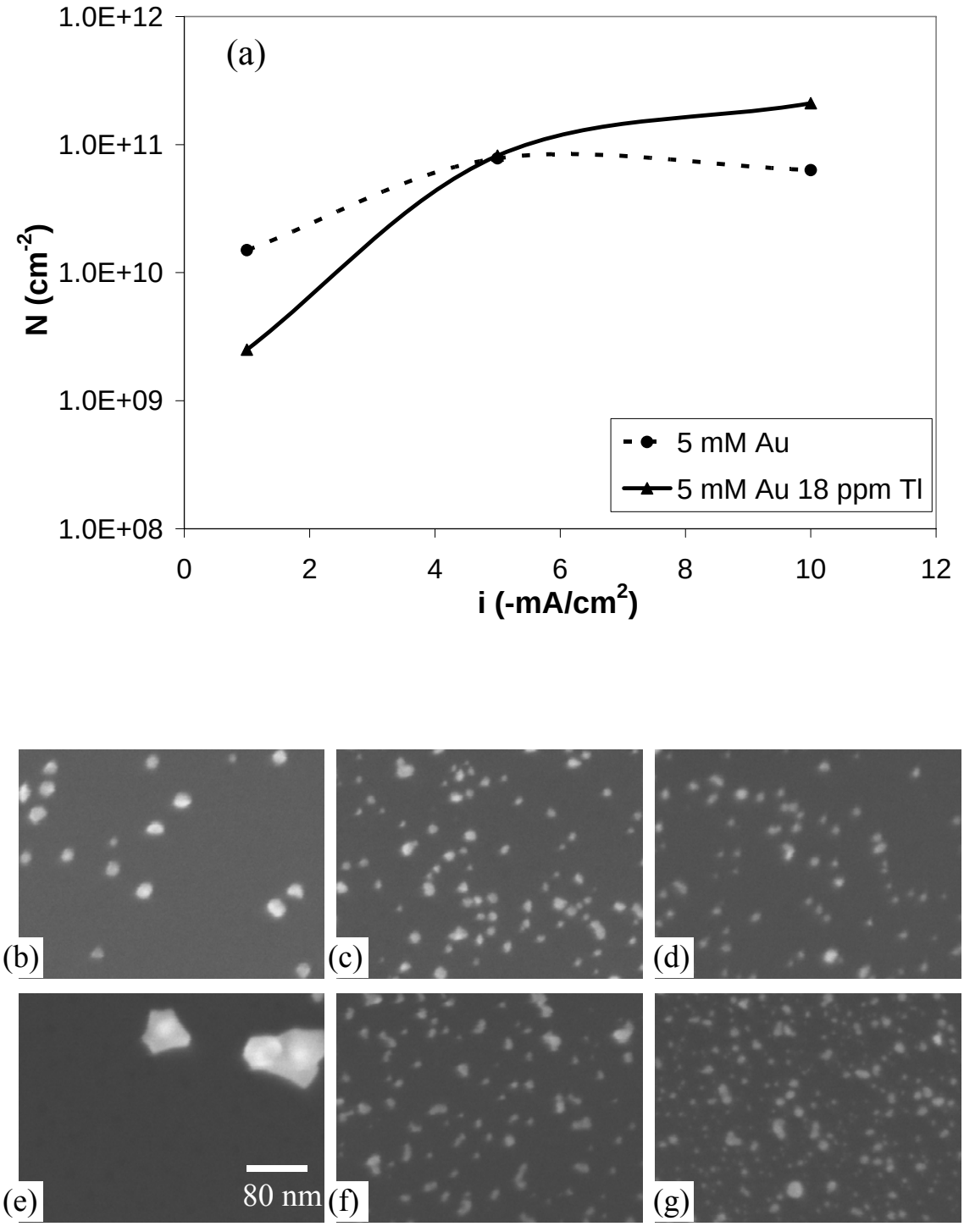

Figure 5 (a - g).

z Email: lili@us.ibm.com

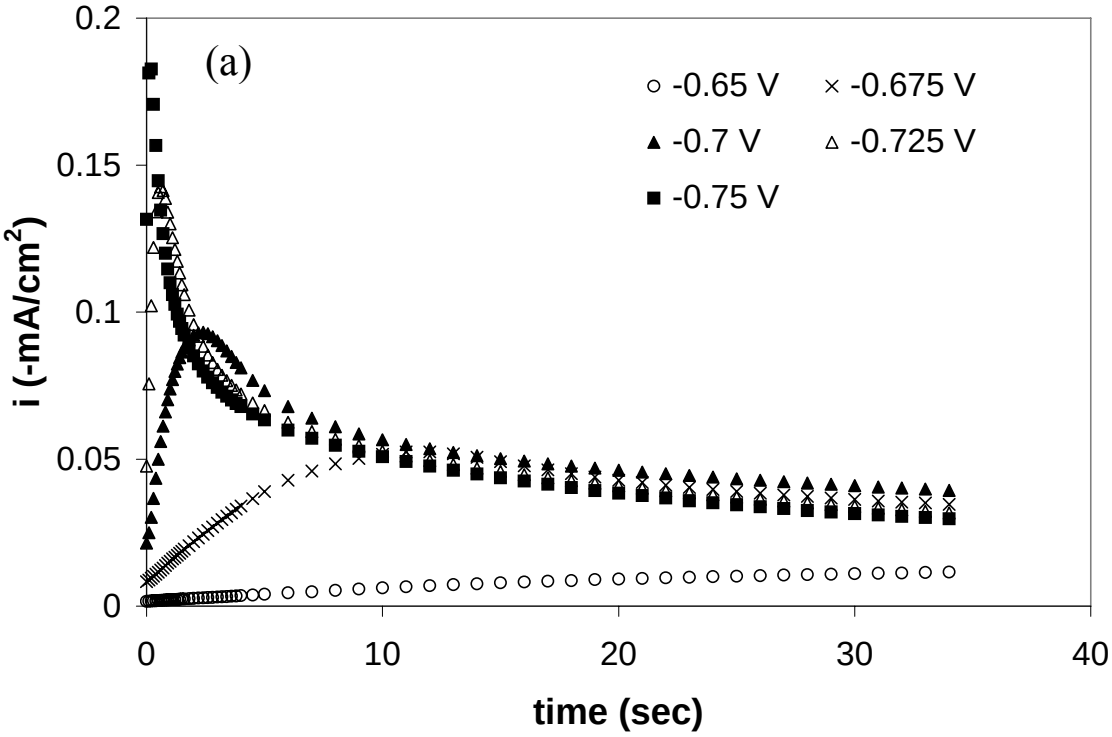

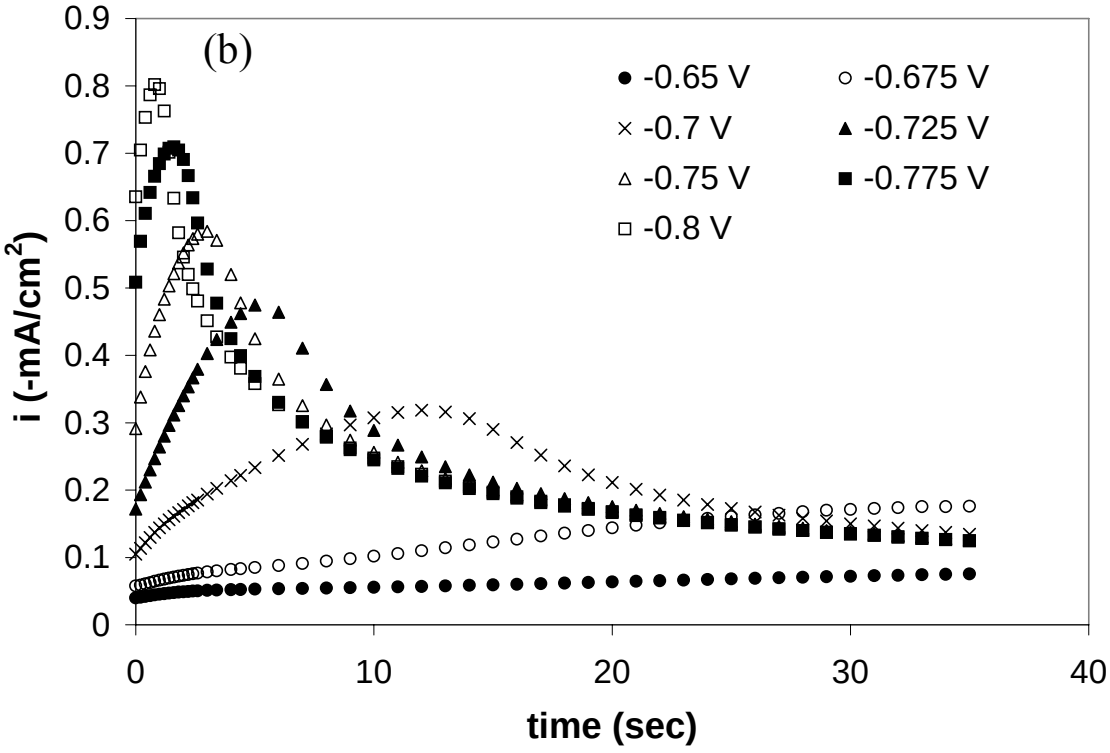

Figure 6 (a, b).

z Email: lili@us.ibm.com

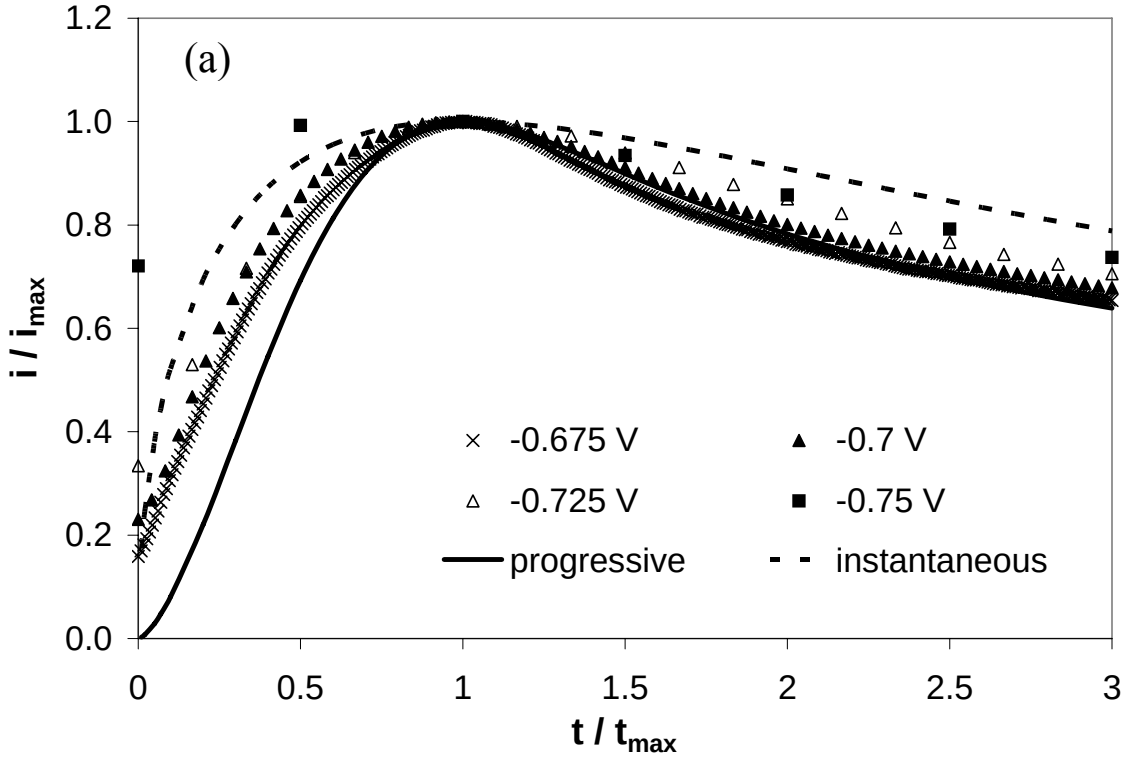

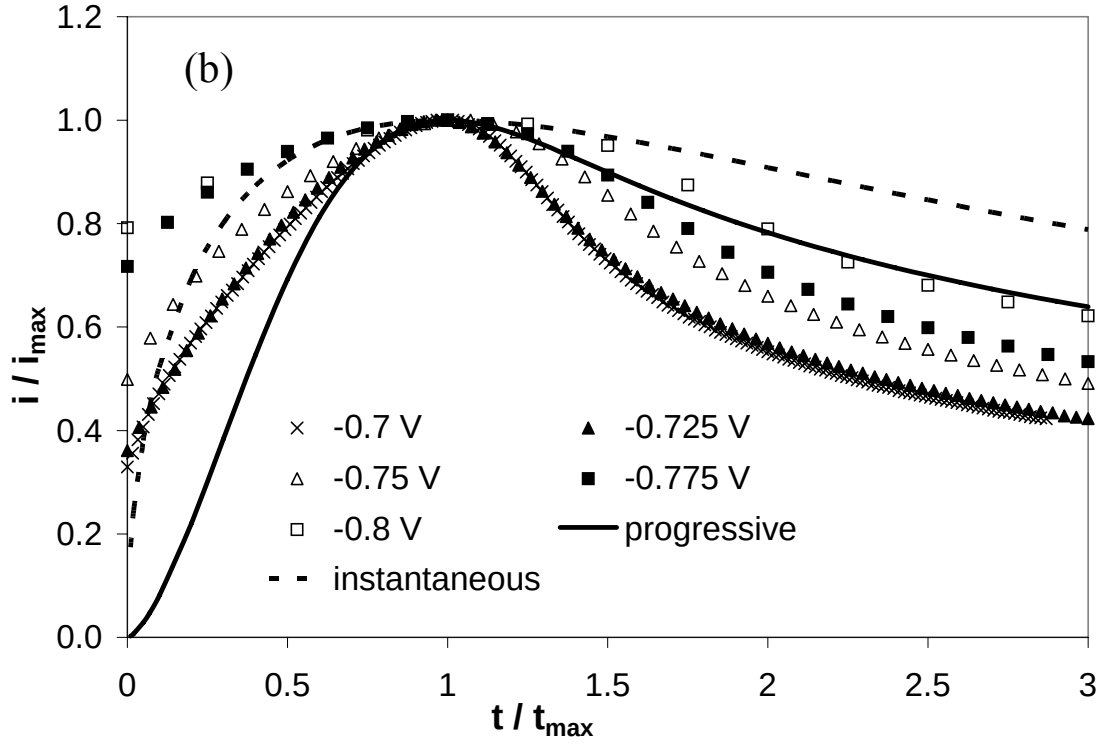

Figure 7 (a, b).

[z] Email: lili@us.ibm.com

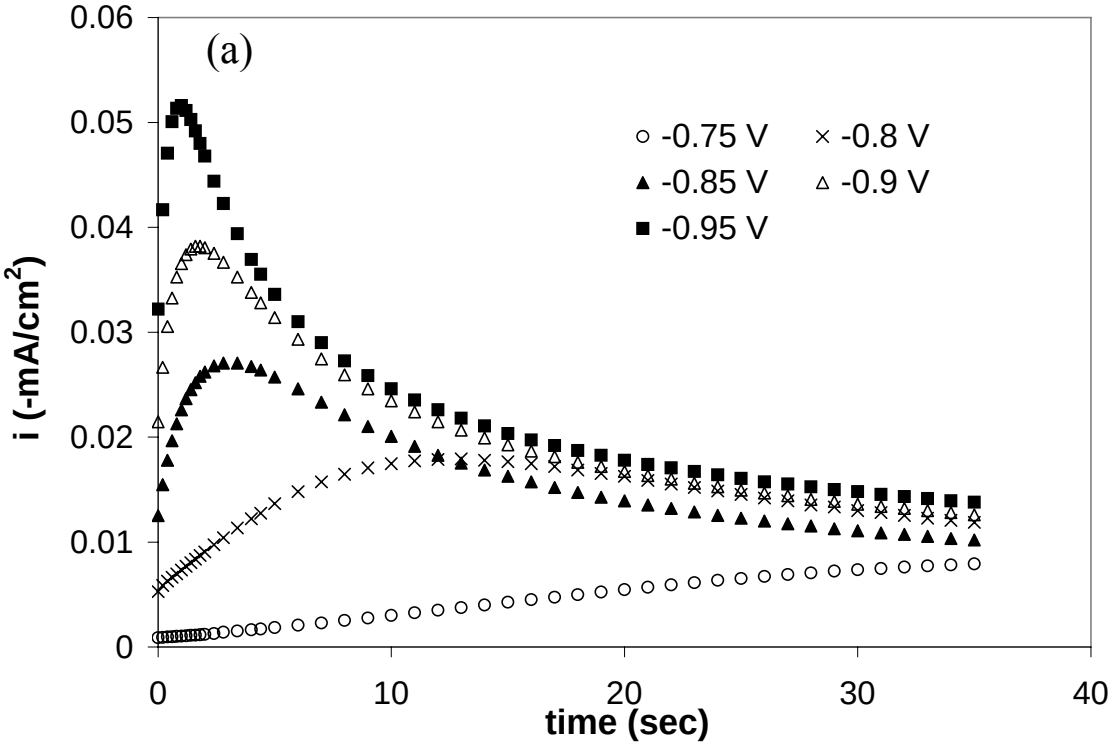

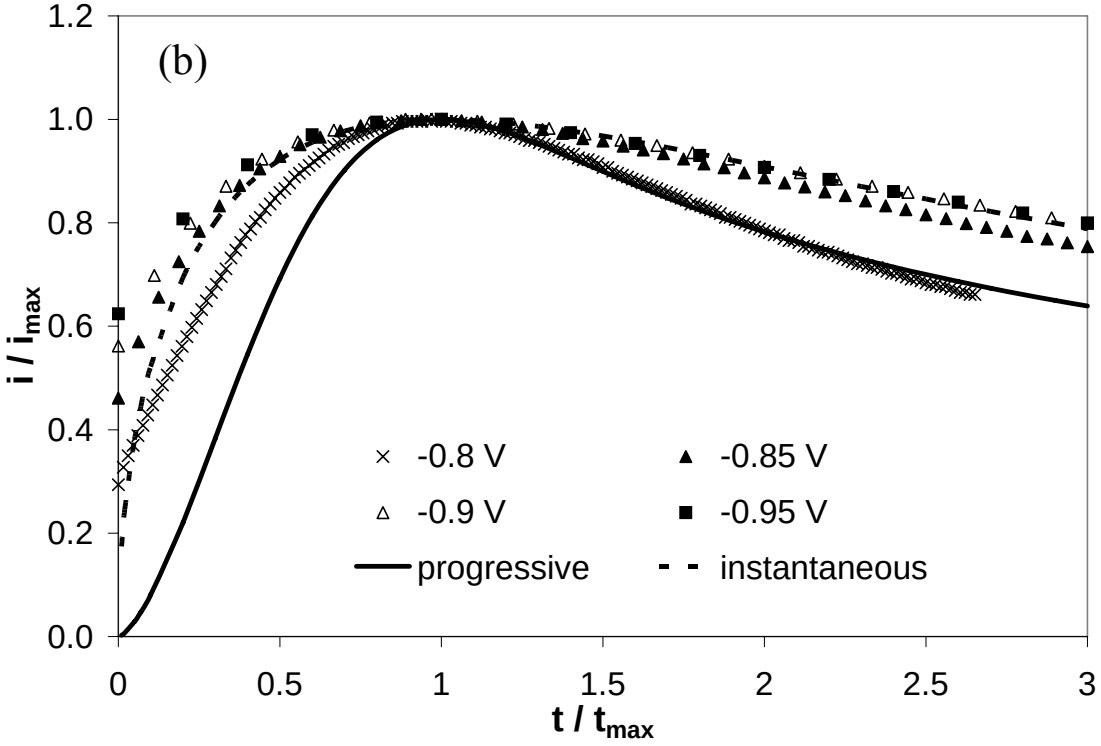

Figure 8 (a, b).

z Email: lili@us.ibm.com

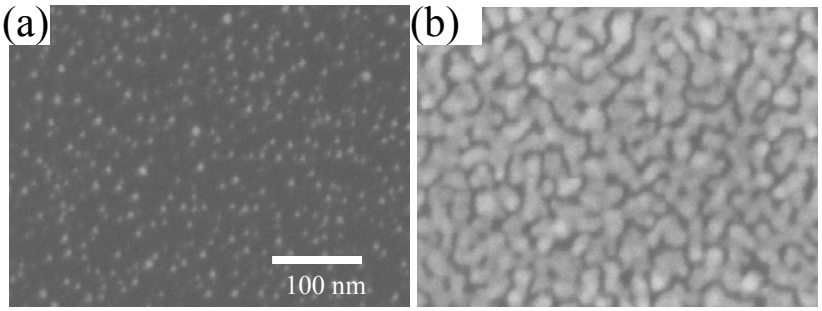

Figure 9.

[z] Email: lili@us.ibm.com